Pergamon

Tetrahedron, Vol. 52, No. 43, pp. 13721-13732, 1996

0040-4020/96 $15.00 + 0.00

PII: S0040-4020(96)00825-3

A Theoretical Investigation on the Reactivity of 6-amino-3-methylpyrimidin-4(3H)-ones Towards DMAD. Tandem Diels-Alder Retro Diels-Alder (DA/RDA) Reaction.

Justo Cobo, Manuel Melguizo, Manuel Nogueras, Adolfo Sánchez*
Química Orgánica. Universidad de Jaén. E-23071 Jaén (Spain).

José A. Dobado and Marco Nonella*
Biochemisches Institut der Universität Zürich.
Winterthurerstr. 190. CH-8057 Zürich (Switzerland).

Abstract: The reactivity of 6-aminopyrimidin-4(3H)-ones towards DMAD is successfully explained by theoretical investigation (PM3 semiempirical methods). All the PM3 results (activation energies (AE) for the transition states and the heat of formation (ΔH) for the products) support our previous experimental work [J. Cobo *et all. Synlett.* **1993**, 4, 297-299; *Tetrahedron* **1994**, 50, 10345-10354]. In those reactions two main products were obtained: the pyridine derivatives **5** as major ones, which are formed by a tandem DA/RDA reaction with extrusion of the methylisocyanate fragment; and 5-ethenylpyrimidin-4(3H)-ones **10** as minor ones, which arised from a Michael addition, being in competition with the above normal DA. Copyright © 1996 Elsevier Science Ltd

INTRODUCTION

Since the pioneering investigations on the participation of oxazoles as azadienes in hetero Diels-Alder (HDA) reactions[1,2], there has been a growing interest in the study of other heteroaromatic systems as azadienes.[3,4] This resulted in the development of synthetic applications and novel synthetic strategies which incorporate different heteroaromatic rings in elegant and straightforward preparations of complex heterocyclic systems.[5,6]

In previous works[7,8], we described the experimental results for the reaction of the 6-aminopyrimidin-4(3H)-one derivatives **1a,b** with DMAD, and its synthetic application to obtain pyridine nucleosides **1c-h**.[9]

Main isolated products in those reactions were the corresponding 2-aminopyridine derivatives **5**, (see Scheme 1). Its formation was rationalised as result of a tandem DA/RDA reaction (see Scheme 2): first a normal DA between C_2-C_5 atoms of the pyrimidine ring and DMAD takes place resulting cycloadducts **3**, which subsequently undergo RDA reaction with lost of methylisocyanate to give the isolated pyridines **5**.

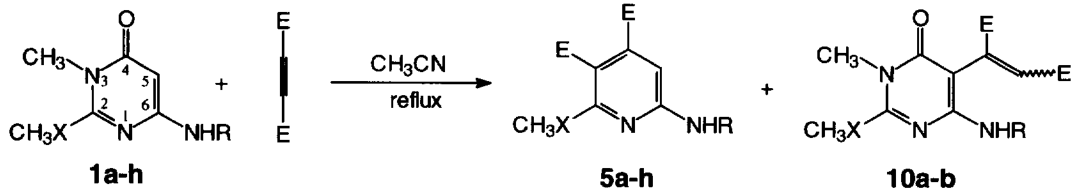

	X	R
a	O	H
b	S	H
c	O	tri-O-acetyl-β-D-xilopyranoside
d	O	tetra-O-acetyl-β-D-glucopyranoside
e	S	tri-O-acetyl-β-D-xilopyranoside
f	S	tetra-O-acetyl-β-D-glucopyranoside
g	O	tri-O-acetyl-β-D-ribofuranoside
h	O	tri-O-acetyl-β-D-ribofuranoside

E = COOCH3

Scheme 1

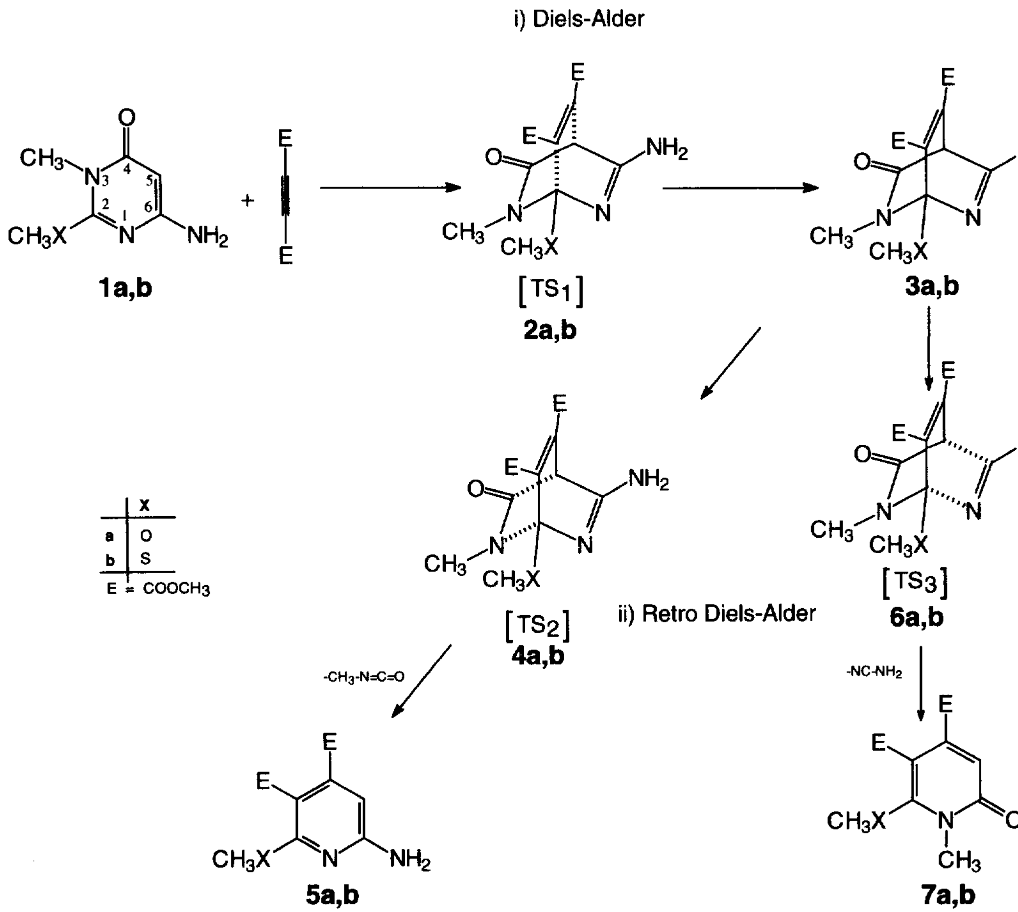

Scheme 2: General scheme for the tandem DA/RDA reaction

All the above reveals some interesting features:

(i).- it is worth noting the ability of compounds **1** to participate as 2-azadienes in normal electron demand DA reaction towards DMAD under mild conditions. Few works dealing with normal DA reaction on pyrimidines as azadienes have been reported[10,11], while most of the literature describe inverse electron demand DA reaction, in clear accordance with the intrinsic electron deficient character of the pyrimidine nucleus.

(ii).- in view of the existing literature[12] two different RDA reactions from the cycloadducts intermediates **3a** and **3b** are expected, as depicted in Scheme 2: one leading to the pyridine derivatives **5a** and **5b** by extrusion of methylisocyanate, and another giving the 2-pyridones **7a** and **7b** by extrusion of cyanamide; however only the former possibility was experimentally observed.

(iii).- the Michael adducts, **10a** and **10b** were also isolated as minor products. (see Scheme 1)

Although the all-carbon DA reaction have been extensively studied in the past (for a recent review see ref. 13), only little is known about HDA reactions.[14-28] The aim of the present work is to provide a theoretical basis for the understanding of HDA reactions of pyrimidines.

Employing the two pyrimidines **1a** and **1b** as simple model molecules (this enables considerable savings in computer time in comparison with more complex glycosylaminopyrimidine derivatives **1c-h**)., which show all the reactivity features of the whole series **1**, we report theoretical results of structures of transition states for the DA, RDA and Michael addition reactions. Furthermore, estimates for activation barriers and reaction enthalpies are given.

The large size of the systems under consideration is prohibitive for using other quantum chemical methods (i.e. *ab initio* or density functional methods) than semiempirical ones. The applied PM3 method has proved to give good results compared to *ab initio* calculations in the study of heterocycles[29] and in the scope of HDA reaction[27]. In our case a direct comparison with experiment is available for checking the theoretical results.

COMPUTATIONAL METHODS

Semiempirical calculations have been carried out with the GAUSSIAN94 package of programs[30] using the PM3 Hamiltonian.[31,32]

All the stationary points were fully optimised without imposing any geometrical constraints. Optimised structures of transition states (TS) were determined with the default TS search method within the GAUSSIAN94. After optimisation of all structures vibrational analysis have been carried out in order to check for the nature of the stationary points. The transition state are defined by exactly one imaginary frequency.

All the energies were corrected for the zero-point vibrational energy (ZPVE) contribution. We also checked the vibrational modes to corroborate that the corresponding negative vibration belongs to the desired transition state. Different orientations for the -XMe (X=O,S) and -COOMe groups were tested to avoid other relative minima. The ring puckering analysis[33] was performed using the COMPUC program.[34,35]

RESULTS AND DISCUSSION

Characterisation of the Transition States (TS) and Products

The transition states **2a, 2b**, **4a, 4b, 6a,** and **6b** (Figure 1) have been fully optimised in order to a better understand the tandem DA/RDA reactions (see Scheme 2), as well as the cycloadduct intermediates **3a** and **3b** (Figure 1) and the products **5a**, **5b** and **7a**, **7b** (Figure 2). Structural parameters of all optimised geometries are listed in Table 1. Very similar structures are found for the a and b series, therefore, the pictures do not include the corresponding b structures.

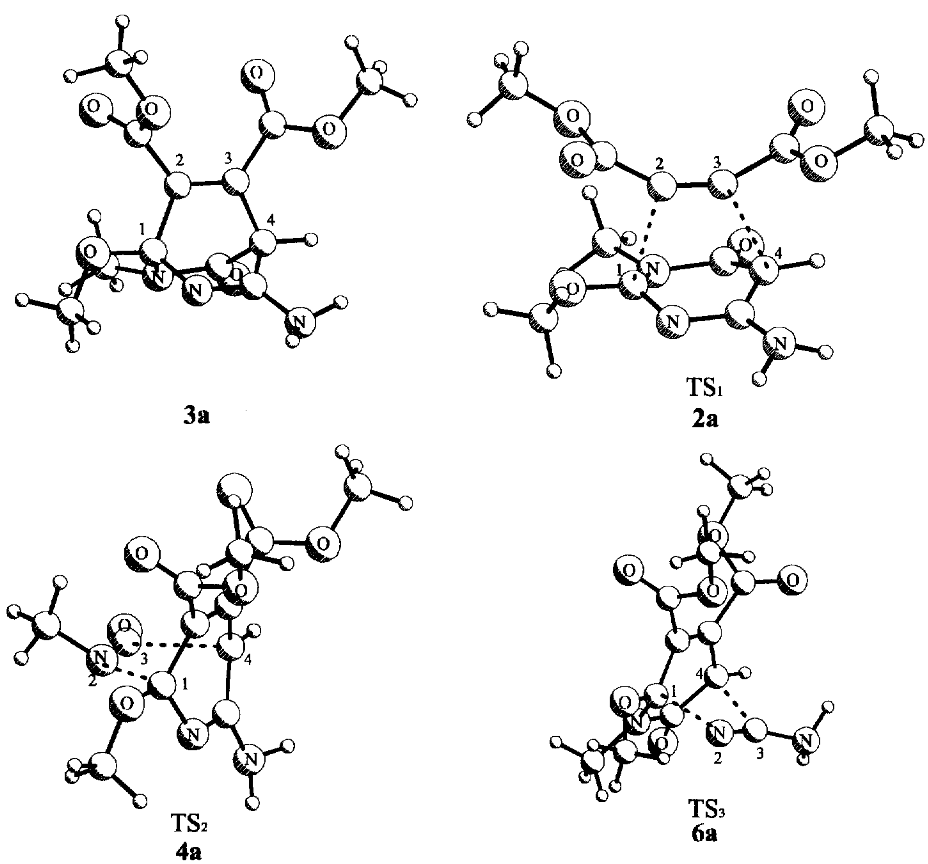

Figure 1: Cycloadduct (**3a**) and TS structures for the DA (**2a**) and RDA (**4a** and **6a**) reactions.

The first TSs (**2a** and **2b**) correspond to the approach of DMAD towards **1a** and **1b** in a concerted DA reaction. These TSs present a low degree of asynchronicity (r_2-r_1, see Table 1) with values c.a. 0.1 Å.

According to the geometrical parameters of Table 1 starting structures **1a** and **1b** are better conserved in TSs **2a** and **2b** than in the cycloadducts intermediates **3a** and **3b**. Comparison of the puckering amplitude q_2 of structures **2a** and **3a** reveals values of 0.39 and 0.82, respectively.

The DA TSs (**2a** and **2b**) evolve to the intermediates (**3a** and **3b**). Besides the back reaction which involves the same TSs **2a** and **2b**, intermediates **3a** and **3b** undergo the two possible RDA reactions resulting in either methylisocyanate or cyanamide extrusions. TSs **4a b** and **6a,b** corresponding to these RDA reactions have been also analysed theoretically.

The main characteristics of those TSs (**4a** and **4b,** and **6a** and **6b**) are:

(i) larger asynchronicity than for **2a** and **2b** (r_1 and r_2 bond lengths of c.a 1.8-1.9 and c.a 2.2-2.3 Å respectively);

(ii) closer similarity of these TSs to the cycloadduct **3a** and **3b** than to the final products (**5a, 5b**, and **7a**, **7b**).

Table 1: PM3 selected geometrical parameters (r_1, r_2, α_1, α_2, ω), imaginary frequency, puckering parameters (q_2, ϕ_2 and q_3) and dipole moment for TSs (**2a,b**, **4a,b**, **6a,b** and **8a,b**) and intermediates (**3a,b** and **9a,b**).

	r_1[a] (Å)	r_2[a] (Å)	α_1[a] (degree)	α_2[a] (degree)	ω[a] (degree)	frequency (cm^{-1})	q_2 (Å)	ϕ_2 (degree)	q_3 (Å)	μ (debye)
2a	2.229	2.137	104.3	114.2	0.5	615 **i**	0.394	58.2	0.012	1.334
2b	2.225	2.124	104.3	115.3	-0.3	658 **i**	0.390	58.4	0.001	1.430
3a	1.545	1.517	112.6	113.7	-1.4		0.825	62.8	0.027	1.833
3b	1.536	1.515	113.1	114.1	-1.4		0.826	62.5	0.021	2.066
4a	1.882	2.232	114.8	102.9	4.1	628 **i**	0.432	239.9	-0.340	1.057
4b	1.871	2.231	115.0	103.1	7.4	675 **i**	0.430	241.0	-0.320	1.216
6a	1.825	2.281	120.4	102.1	-2.8	579 **i**	0.464	235.9	-0.660	1.221
6b	1.852	2.230	119.3	103.9	-1.9	569 **i**	0.467	235.8	-0.570	1.333
8a		1.828		117.6	10.2	546 **i**	0.121	229.1	0.071	2.014
8b		1.810		118.2	9.0	548 **i**	0.164	224.0	0.080	2.096
9a		1.519		115.4	26.8		0.220	207.8	0.066	3.221
9b		1.523		116.1	23.4		0.298	216.5	0.098	3.311

[a]bond lenths r_1 (between atoms 1-2), r_2 (between atoms 3-4), angles α_1 and α_2 (∠1-2-3 and ∠2-3-4 respectively) and dihedral angle ω (∠1-2-3-4), the numbering is depicted in Figures 1 and 3.

The conformation of the pyrimidine ring is planar for the structures **1a-b**, and for the pyridines **5a-b** and **7a-b**; while a boat conformation (ϕ_2 of 60 or 240°) is adopted with atoms C_2 and C_5 pointing out of plane for structures **2a-b**, **3a-b**, **4a-b** and **6a-b**. For a quantitative characterisation of the ring conformation, the corresponding puckering parameters are listed in Table 2. The puckering amplitude q_2 gives us a measure for the deviation from the planarity of the ring systems. The largest q_2 values are found in the case of the cycloadduct **3a** and **3b** (c.a. 0.8 Å), followed by structures **4a-b** and **6a-b** with similar values of q_2 around 0.4 Å.

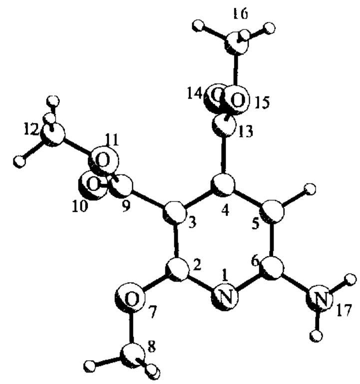

5a

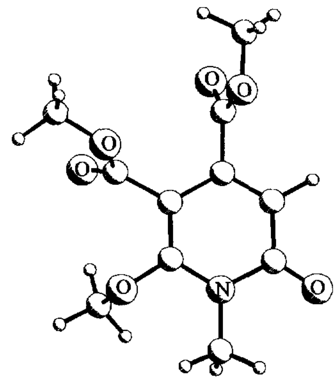

7a

Figure 2: Products (**5a** and **7a**) for the DA/RDA reaction

Table 2: PM3 and X-ray geometrical parameters for structures **5a** and **5b**.

bond lengths‡ (Å)	**PM3**	**Exptl.**¶	**PM3**	**Exptl.**¶	**angles**‡ (degrees)	**PM3**	**Exptl.**¶	**PM3**	**Exptl.**¶
	Structure **5a**		Structure **5b**			Structure **5a**		Structure **5b**	
N_1-C_6	1,367	-0,022	1,362	-0,022	∠C_6-N_1-C_2	118,40	0,19	120,58	-1,64
N_1-C_2	1,359	-0,034	1,359	-0,019	∠N_1-C_6-N_{17}	115,84	1,19	116,21	1,66
N_{17}-C_6	1,410	-0,066	1,413	-0,066	∠N_{17}-C_6-C_5	122,14	-1,24	122,17	0,00
C_6-C_5	1,408	-0,003	1,408	-0,002	∠N_1-C_6-C_5	121,44	0,65	121,87	-1,93
C_5-C_4	1,392	-0,024	1,389	-0,024	∠C_6-C_5-C_4	118,74	-0,60	118,10	0,35
C_4-C_3	1,397	0,006	1,401	0,008	∠C_5-C_4-C_3	120,56	1,08	120,59	0,38
C_4-C_{13}	1,496	0,015	1,496	0,006	∠C_5-C_4-C_{13}	117,77	-1,70	117,60	-1,11
O_{14}-C_{13}	1,213	-0,014	1,214	-0,009	∠C_3-C_4-C_{13}	121,67	0,49	121,81	0,62
O_{15}-C_{13}	1,367	-0,045	1,366	-0,041	∠O_{14}-C_{13}-O_{15}	120,00	5,20	120,23	4,59
O_{15}-C_{16}	1,412	0,036	1,412	0,031	∠O_{14}-C_{13}-C_4	127,53	-4,53	127,30	-3,07
C_3-C_2	1,415	0,001	1,409	0,004	∠O_{15}-C_{13}-C_4	112,46	-1,00	112,45	-1,74
C_3-C_9	1,489	-0,018	1,495	-0,016	∠C_{13}-O_{15}-C_{16}	118,46	-1,96	118,54	-2,51
O_{10}-C_9	1,211	0,002	1,212	-0,006	∠C_4 -C_3 -C_2	117,41	-2,22	118,88	-2,70
O_{11}-C_9	1,370	-0,053	1,367	-0,035	∠C_4-C_3-C_9	122,48	-4,37	119,61	-2,92
O_{11}-C_{12}	1,412	0,037	1,412	0,038	∠C_2-C_3-C_9	120,12	6,49	121,51	5,56
X_7-C_2	1,363	-0,025	1,771	-0,005	∠O_{10}-C_9-O_{11}	119,98	2,46	120,10	2,89
X_7-C_8	1,413	0,029	1,803	-0,007	∠O_{10}-C_9-C_3	127,61	-6,21	127,53	-5,08
					∠O_{11}-C_9-C_3	112,40	3,77	112,44	2,12
					∠C_9-O_{11}-C_{12}	120,01	-4,16	120,10	-4,78
					∠N_1-C_2-C_3	123,00	1,34	120,40	2,71
					∠N_1-C_2-X_7	119,16	-1,63	118,33	-2,79
					∠X_7-C_2-C_3	117,82	0,31	121,27	0,07
					∠C_2-X_7-C_8	118,58	-1,47	106,12	-4,00

‡X=O and S for structures **5a** and **5b** respectively (the atoms numbering is depicted in Figure 2).
¶Difference between the PM3 values and the crystallographic data of ref.[36]

In order to check the PM3 geometrical parameters with the available experimental data[36], characteristic geometrical parameters (bond length and angles of the heavy atoms skeleton) of the structures **5a** and **5b** are compared to X-ray data in Table 2.

The largest difference is found in the bond length corresponded to the N_{17}–C_6 bond (see Figure 2), where the x-ray data gave a bond length which is by 0.066Å shorter than that predicted by the PM3 method. This difference could be explained by the formation of intermolecular hydrogen bonds between amino and oxo groups in the crystal. The largest discrepancies found in bond angles is about 6°. This comparison confirms that the PM3 geometries obtained for this kind of heterocycles are acceptable.

Energetics for the global process

The PM3 activation energies (AE) of the TSs and reaction enthalpies (ΔH) for the products are listed in Table 3 for each step of the global reaction shown in Scheme 2. For further comparison we have also included the experimental yield in acetonitrile in that table.

Table 3: PM3 activation energies (AE) and reaction enthalpies (ΔH) for the tandem DA/RDA and Michael addition reactions (kcal/mol)*.

	Diels-Alder		Retro Diels-Alder				
	AE_1	ΔH_1	AE_2	ΔH_2	Yields[‡]	AE_3	ΔH_3
a	39.6(40.0)	-22.8(-19.4)	40.0(37.4)	-3.6(-6.9)	79% (4h)	50.7(48.1)	13.7(10.2)
b	45.1(45.3)	-17.7(-14.5)	41.1(38.5)	-9.5(-12.7)	64% (21h)	51.9(49.1)	10.2(6.8)

	Michael Addition		
	AE_4	ΔH_4	Yields[‡]
a	30.3(30.2)	22.4(24.3)	16% (4h)
b	31.8(31.7)	26.2(27.4)	24 % (21h)

[‡]Experimental reaction yields and time of reaction in acetonitrile from ref.[8]
*the values in parentheses are corrected for the ZPVE contribution.

The first DA reaction exhibits an activation energy AE_1 and reaction enthalpy ΔH_1 of 40.0 and -19.4 kcal/mol for structure **a**, and 45.3 and -14.5 kcal/mol for structure **b** respectively (values corrected for the ZPVE contribution). The cycloadduct, thus, is favored by 19.4 and 14.5 kcal/mol for **a** and **b** respectively over their corresponding precursors. After the cycloadduct formation, the reaction coordinate in order to reach product **5a** exhibits an activation energy and reaction enthalpy 37.4 and -6.9 for **a** and 38.5 and -12.7 kcal/mol for **b** respectively. The reaction, thus, has its equilibrium on the product side. In contrast to these findings the alternative path consisting in extrusion of cyanamide shows a high activation barriers AE_3 of 48.1 and 49.1 kcal/mol for structure **a** and **b** respectively, and positive reaction enthalpies ΔH_3 of 10.2 and 6.8 kcal/mol for **a** and **b** respectively. This reaction, therefore, has its equilibrium on the adduct side.

A global comparison of the different DA/RDA paths shows:

(i) the theoretical results of the DA/RDA towards the formation of **5a,b** do not definitively support a rate determinant step for this reaction, although after ZPVE correction AE_2 is slightly lower than AE_1 resulting in a faster formation of the products **5a** and **5b** compared to the formation of **3a** and **3b**. This agrees with the experimental observation that no isolation of intermediates **3a** and **3b** was possible, most likely because these intermediates immediately underwent the cycloadduct opening.

(ii) there is no experimental evidence for the cyanamide extrusion to take place. The PM3 results clearly support this finding in terms of an activation energy which is c.a. 10 kcal/mol higher than AE_2 and by the positive reaction enthalpy indicating a thermodynamically unfavourable process.

(iii) experimentally, the structures **a** are favoured against **b** with respect to the formation of products **5a** and **5b** (see Table 3). These findings are supported by the larger AE_1 of **a** compared to that of **b**.

Analysis of the reaction products reveals an additional component arising from a Michael-type addition which competes the tandem DA/RDA reaction. For this competitive reaction, our calculations revealed a path leading to intermediate **9a,b** (Scheme 3) through a TS **8a,b** (Figure 3) with an activation energy AE_4 of 30.2 and 31.7 kcal/mol from **1a** and **1b** respectively, which , thus, is considerably lower than that for the DA reaction (AE_1 of 40.0 and 45.3 kcal/mol for **a** and **b**).

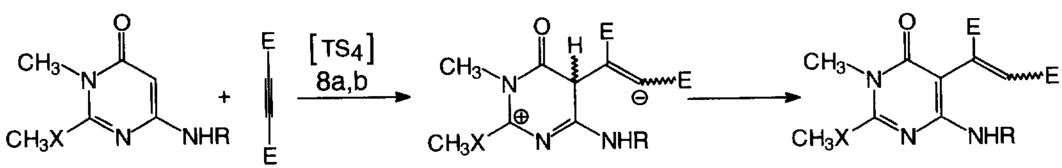

Scheme 3

The zwitterionic character of these intermediates, however, makes their formation largely endothermic, as is indicated by the reaction enthalpy ΔH_4 value of 24.3 and 27.4 kcal/mol (for **9a** and **9b**). This result explains why this pathway is disfavoured against the DA/RDA reaction under the conditions indicated in Figure 1 (acetonitrile as solvent). That is, intermediates **9a,b** evolve to the Michael addition products, **10a,b**, through a prototropy for which the solvent molecules play a determinant role with respect to the proton transfer step. Thus, the ability of the Michael-type addition process to compete with the DA/RDA pathway depends directly on the ability of the solvent to assist proton transfer. This is coherent with the experimental finding that reaction between **1a** and DMAD in acetonitrile yielded 79% of **5a** and 16% of **10a** (see Scheme 1), while the same reaction ran in a solvent that favours proton transfer, like methanol, gave **10a** as the main product (53% isolated) together with 6% of a pyrrolo[3,4-*c*]pyridine derivative **11a** (see Scheme 4) and product from DA/RDA reaction (**5a**) was not isolated or even detected by t.l.c.[37]

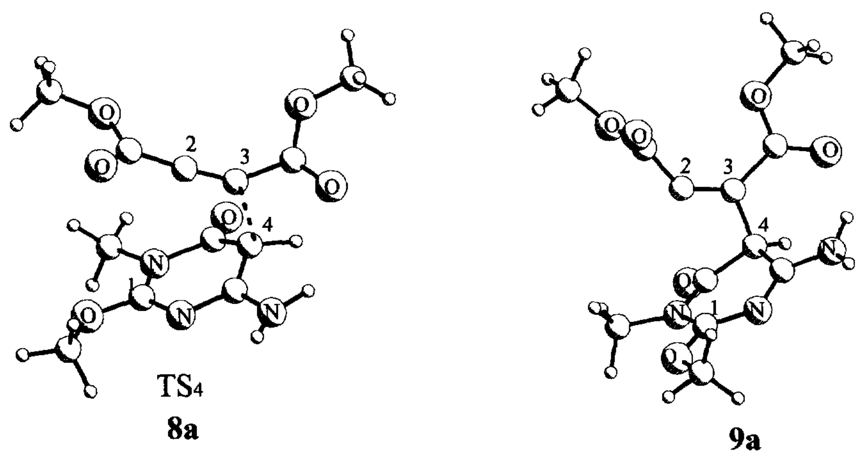

Figure 3: TS (**8a**) and intermediate (**9a**) structures for the Michael addition reaction.

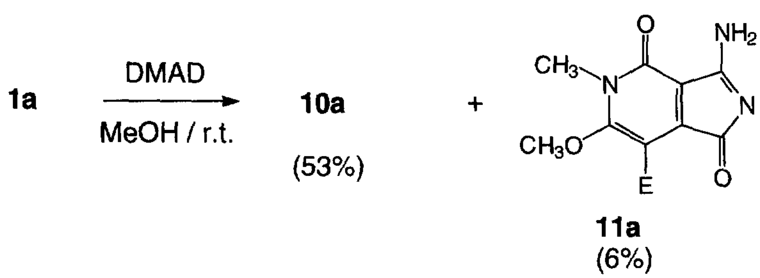

Scheme 4

CONCLUSIONS

The PM3 geometrical parameters for the structures **5a** and **5b** are in a good agreement with previously reported crystallographic data.

The theoretical PM3 results corroborate the experimental findings explaining a reaction mechanism of 6-aminopyrimidin-4(3H)-one derivatives towards DMAD that consists in a tandem Diels-Alder Retro Diels-Alder reaction (DA/RDA).

The calculations furthermore explain that an extrusion of the cyanamide fragment to yield products **7** is an unfavourable process compared to the first step of the DA/RDA sequence, with an activation barrier AE_4 about 10 kcal/mol lower than that of the DA reaction.

The Michael addition reaction proceeds with the formation of a zwitterion intermediate and is thermodynamically unfavourable.

The experimentally found reactivity order (**a**) > (**b**) with respect to the tandem DA/RDA reaction is correctly reproduced by the calculation.

ACKNOWLEDGEMENTS

Computing time has been provided by the Rechenzentrum der Universität Zürich.

REFERENCES

1 Kondrat'eva, G.Y. *Chem. Abstr.* **1958**, 52, 6345.

2 Kondrat'eva, G.Y. *Izv. Akad. Nauk SSSR* **1959**, 484.

3 Boger, D. *Chem. Rev.* **1986**, 86, 781.

4 Boger, D. *Hetero Diels-Alder Methodology in Organic Synthesis*, Vol. *47* of Organic Chemistry; Academic Press, New York, **1987**.

5 Boger, D.; Kochany, M. *J. Org. Chem.* **1994**, 59, 4950.

6 Boger, D.; Honda, T.; Dang, Q. *J. Am. Chem. Soc.* **1994**, 116, 5619.

7 Cobo, J.; Melguizo, M.; Nogueras, M.; Sanchez, A.*Synlett.* **1993**, 4, 297.

8 Cobo, J.; García, C.; Melguizo, M.; Nogueras, M.; Sanchez, A. *Tetrahedron* **1994**, 50, 10345.

9 Cobo, J.; Melguizo, M.; Nogueras, M.; Sanchez, A. *Tetrahedron* **1996**, 52, 5845.

10 Kashima, C.; Shimizu, M.; Omote, Y. *Chem. Pharm. Bull* **1987**, 35, 2694.

11 Machin, P. J.; Porter, A.; Sammes, P. *J. Chem. Soc.* , *Perkin Trans. 1* **1973**, 404

12 Stolle, W. A. W.; Marcelis, A. T. M.; van der Plas, H. C. *Tetrahedron* **1992**, 48, 1657.

13 Houk, K. N.; Gonzalez, J.; Li, Y. *Acc. Chem. Res.* **1995**, 28, 81.

14 Neder, B.; Bailey, T. R.; Franck, R. W.; Weinreb, S. M. *J. Am. Chem. Soc.* **1981**, 103, 7573

15 Le, I.; Han, E. S.; Choi, J. Y. *J. Comput. Chem.* **1984**, 5, 606

16 Clennan, E. L.; Earlywine, A. D. *J. Am. Chem. Soc.* **1987**, 109, 7104

17 Jensen, F.; Foote, C. S. *J. Am. Chem. Soc.* **1987**, 109, 6376

18 Birkinshaw, T. N.; Tabor, A. B.; Kayne, P.; Mayne, P. M.; Raithby, P. R. *J. Chem. Soc. Chem. Commun.* **1988**, 1599

19 O'Shea, K.; Foote, C. S. *J. Am. Chem. Soc.* **1988**, 110, 7167

20 Tietze, L. F.; Fennen, J.; Ernst, A. *Angew. Chem. ,Int. Ed. Engl.* **1989**, 28, 1371

21 Le Coz, L.; Veyrat-Martin, C.; Wartski, L.; et al. *J. Org. Chem.* **1990**, 55, 4870.

22 Coxon, J. M.; McDonald, D. Q. *Tetrahedron Lett.* **1992**, 33, 3673

23 Dau, M. E. T. H.; Flament, J.-P.; Lefour, J.-M.; Riche, C.; Grieson, D. S. *Tetrahedron Lett.* **1992**, 33,

24 Gonzalez, J.; Houk, K. N. *J. Org. Chem.* **1992**, 57, 3031.

25 Jursic, B. S.; Zdravkovski, Z. *J. Heterocycl. Chem.* **1994**, 31, 1429

26 Tietze, L. F.; Schulz, G. *Liebigs Annalen* **1995**, 1921.

27 Domingo, L. R.; Jones, R. A.; Picher, M. T.; Sepulveda-Arques, J. *Tetrahedron* **1995**, 51, 8739.

28 Jursic, B. S.; Zdravkovski, Z. *J. Phys. Org. Chem.* **1994**, 7, 641, and references therein.

29 Dobado, J. A.; Molina, J.; Rodriguez-Espinosa, M. *J. Mol. Struct. (Theochem)* **1994**, 303, 205.

30 GAUSSIAN 94, rev b.3. Frisch, M. J.; Trucks, G. W.; Schlegel, H. B.; Gill, P. M. W.; Johnson, B. G.; Robb, M. A.; Cheeseman, J. R.; Keith, T.; Petersson, G. A.; Montgomery, J. A.; Raghavachari, K.; Al-Laham, M. A.; Zakrzewski, V. G.; Ortiz, J. V.; Foresman, J. B.; Peng, C. Y.; Ayala, P. Y.; Chen, W.; Wong, M. W.; Andres, J. L.; Replogle, E. S.; Gomperts, R.; Martin, R. L.; Fox, D. J.; Binkley, J. S.; Defrees, D. J.; Baker, J.; Stewart, J. J. P.; Head-Gordon, M.; Gonzalez, C.; Pople, J. A. Gaussian Inc. 1995 Pittsburg PA.

31 Stewart, J. J. P. *J. Comp. Chem.* **1989**, 10, 209

32 Stewart, J. J. P. *J. Comp. Chem.* **1989**, 10, 221

33 Cremer, D.; Pople, J. A. *J. Am. Chem. Soc.* **1975**, 97, 1354

34 Stahl, K. *Inorg. Chim. Acta* **1983**, 75, 85

35 Evans, D. G.; Boeyens, J. C. *Acta Crystallogr., Sect. B* **1989**, 45, 581

36 Low, J. N.; Ferguson, G.; Cobo, J.; Melguizo, M.; Nogueras, M.; Sanchez, A. *Acta Crystallographica - Section C - Crystal Structure Communications* **1996**, 52, 143.

37 García, C., Melguizo, M.; Nogueras, M.; Sánchez, A. *Communications to the XIVth European Colloquium on Heterocyclic Chemistry, Toledo (Spain) October 13,* **1990** *(book of Abstracts pag 167).*

(*Received in UK* 1 *August* 1996; *revised* 11 *September* 1996; *accepted* 12 *September* 1996)